Sainmatika: Jurnal Ilmiah Matematika dan Ilmu Pengetahuan Alam
Volume 21 No. 2, December 2024 DOI 10.31851/sainmatika.v21i2.16068
https://jurnal.univpgri-palembang.ac.id/index.php/sainmatika

Numerical Simulation of Run-Up Wave Using Nonlinear Shallow Water Equations with Staggered Grid at Canti Beach, South Lampung

Dear Michiko Mutiara Noor[1], Maya Himmah Faiqoh[2], Rifky Fauzi[3*]
e-mail: *rifky.fauzi@ma.itera.ac.id

[1,2,3*]*Department of Mathematics, Faculty of Science, Institut Teknologi Sumatera, Lampung, Indonesia*

ABSTRACT

Tsunamis, wave triggered by underwater earthquakes or volcanic eruptions, can achieve significant run-up heights upon reaching shore. Run-up refers to the maximum vertical distance a tsunami wave reaches above the normal sea level. This study employs a numerical model to simulate the run-up wave at Canti Beach, South Lampung Regency, during the 2018 Sunda Strait tsunami. The method approximates solutions to the shallow water model consisting of mass and momentum conservation equations using the finite difference method in staggered grid grids and incorporates the upwind method for nonlinear terms. Bathymetry data from GEBCO was projected in two dimensions using the haversine formula. The numerical scheme includes a wet-dry procedure for simulating run-up waves. Results indicate that waves with a 60-second period and 0.09-meter amplitude create a 40.0195-meter inundation area, although this amplitude is significantly lower than the observed data from the 2018 Sunda Strait tsunami. Additionally, a simulation with a 0.1-meter amplitude results in a 1.8299-meter run-up height, closely matching the observed data. This study demonstrates that nonlinear shallow water equations can effectively estimate run-up height and inundation area at Canti Beach.

Keywords: Tsunami, run up, shallow water equations, finite difference, staggered grid

INTRODUCTION

Indonesia, an archipelago formed by volcanic activity, frequently experiences earthquakes due to its unique geological characteristics (Cummins, et al., 2020). Located on the Pacific Ring of Fire, the country faces a high risk of volcanic eruptions, which can cause significant casualties and economic losses in sectors such as tourism, culinary arts, and agriculture (Campbell, 2022). On December 22, 2018, a tsunami in the Sunda Strait, triggered by the eruption of Mount Anak Krakatau, struck the coast of the Banten and Lampung provinces, causing substantial damage (Sabara, et al., 2021). The five severely affected regencies were Serang, Pandeglang, South Lampung, Pesawaran, and Tanggamus (Tiwi, et al., 2023). Predicting the extent of inundation, or the territory flooded by such events, is crucial when it regarding tsunami modeling. Run-up waves are defined as the highest vertical increase of water over the still water level when waves break to shore (Wang, et al., 2023). The significance of these calculations for assessing coastal risk has been well-documented in earlier studies (Tursina, et al., 2021). For regions like Indonesia, more precise models that can take into account the complex interactions between tsunami waves and coastal topography are still essential.

This study focuses on the run-up wave phenomenon at Canti Beach, employing bathymetric mapping and Nonlinear Shallow Water Equations (SWE) to predict the behavior of tsunami waves (Arifin, 2021). There is a gap in

p-ISSN 1829 586X
e-ISSN 2581-0170

the application of the SWE to the particular coastal dynamics of Canti Beach, despite the fact that other research have used it in a variety of scenarios, including wave propagation (Fauzi & Wiryanto, 2017) and granular landslides (Fauzi & Wiryanto, 2021; Fauzi & Wiryanto, 2023). This research attempts to improve the accuracy of numerical methods for wave propagation by solving the SWE using the Staggered Grid Finite Difference Method, addressing the need to enhance disaster mitigation in Indonesia. The study not only contributes to the understanding of the interaction between tsunami waves and the shoreline but also provides insights crucial for sustainable coastal management and disaster mitigation (Busayo & Kalumba, 2020).

The simulation results highlight the critical role of detailed bathymetric data, such as that provided by the General Bathymetric Chart of the Oceans (GEBCO), in enhancing the accuracy of these models. By projecting this data using the Haversine Formula and processing it with Surfer software to create two-dimensional bathymetric maps, this study aims to simulate wave run-up using real bathymetric data of Pantai Canti and compare the results with field data from the 2018 Sunda Strait Tsunami. In particular, our focus is on determining the wave's frequency and amplitude at the moment of occurrence. Our technique uses the run-up and flooding field data that the Indonesian Meteorology, Climatology, and Geophysical Agency (BMKG) immediately gathered after the tragedy since there are no direct observations of the incoming tsunami waves.

MATERIAL AND METHOD

According to the BMKG Kotabumi survey report from December 2018, the wave run-up height at Canti Beach Pier reached 1.85m and an inundation of 35.45m (Sugiarto, Rudianto, & Somali, 2018). The data points gathered for bathymetric data are shown in Figure 1, which extends from that particular point to the Canti shoreline. The field data for the Sunda Strait tsunami event is presented in Table 1, which includes run-up heights and inundation areas (distance from the shoreline).

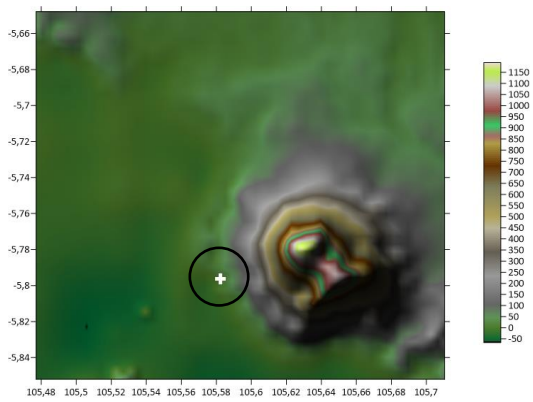

Figure 1. The bathymetric map at Canti Beach with Surfer

Table 1. Survey data on the tsunami at Canti Beach

Latitude	Longitude	Run up height	Inundation area
-5.80014	105.58449	1.85	35.45

Preprocessing 3D Bathymetric Data into 2D via Haversine Formula

The Haversine Formula is a mathematical method commonly used to estimate the distance between two points on the Earth's surface by taking into account the latitude and longitude values of this point (Azdy & Darnis, 2020).

The Haversine formula can be written as follows :

$$d = 2r \cdot sin^{-1}\left(\sqrt{sin^2\left(\frac{\varphi_2 - \varphi_1}{2}\right) + cos(\varphi_1) \cdot cos(\varphi_2) \cdot sin^2\left(\frac{\psi_2 - \psi_1}{1}\right)}\right) \quad (1)$$

where r is the Radius of the Earth (6371000 meters), φ is the Latitude coordinate, ψ is the Longitude coordinate, c is the Calculation of the

intersection axis, d^* is the Distance between two points (meters), and 1 degree is 0.01745 radians.

Table 2. Bathymetric data around the waters of Canti Beach

Bathymetric depth d_0	Distance d^*
-20.8871	0
-21.5681	246.9086
-23.3152	333.5939
-17.1213	406.3287
1.9380	521.2017
25.9675	558.6122
57.3060	606.6714
63.3360	647.4368
71.0811	673.6261
64.9599	1144.5590

Bathymetric depth is the vertical measurement of a point on the underwater surface, such as a seabed, relative to the sea surface. The depth is used in the Haversine Formula to obtain the observation distance value. Table 2 shows the outcomes of these procedures.

However, there is another approach could be used to approximate the bathymetry by using a neural network (Sianturi & Fauzi, 2024).

Numerical Shallow Water Model

In the wave simulation process, a Nonlinear Shallow Water Equation (SWE) Model is used. This SWE is based on the application of nonlinear mass conservation principles and nonlinear momentum conservation principles.

$$h_t + (hu)_x = 0 \quad (2)$$

$$u_t + uu_x + g\eta_x = 0 \quad (3)$$

Boundary conditions on the left consist of incoming waves,

$$\eta(0,t) = A\sin(ft) = A\ sin\left(\frac{2\pi t}{T}\right) \quad (4)$$

and absorbing boundary conditions at $x = 0$,

$$u(0,t) = \sqrt{\frac{g}{d_0}}\ \eta(0,t) \quad (5)$$

This study uses a special grid configuration based on the Arakawa C grid, namely a staggered grid. This grid is different with any other grid system where the variables are located at different locations (Goyman & Shashkin, 2021). On a staggered grid, surface displacement and bathymetry is located at $x_{j+1/2}$, while the water velocity is located at x_j.

Equation (2) is approximated On the interval $[x_j, x_{j+1}]$. The finite difference

$$\frac{\eta_{j+\frac{1}{2}}^{n+1} - \eta_{j+\frac{1}{2}}^{n}}{\Delta t} + \frac{q_{j+1}^n - q_j^n}{\Delta x} = 0$$

where $q|_j^n = \hat{h}_j^n \cdot u_j^n$. The upwind approximation is used to approximate water depth in the full grid x_j (Pudjaprasetya, 2018), namely

$$q_j = \begin{cases} \hat{h}_{j-\frac{1}{2}} \cdot u_j, & u_j \geq 0 \\ \hat{h}_{j+\frac{1}{2}} \cdot u_j, & u_j < 0 \end{cases}$$

Equation (3) is approximated in the interval $[x_{j-1/2}, x_{j+1/2}]$, namely

$$\frac{du_j}{dt} + g\frac{\eta_{j+1/2}^{n+1} - \eta_{j-1/2}^{n+1}}{\Delta x} + (uu)_x|_j^n = 0 \quad (6)$$

The positive total water depth $u_{j-1/2}$ is calculated using equation (6) only if the calculated interval is wet. The upwind method considers the direction of fluid flow when calculating gradients, giving more weight to values from the "upwind" direction (opposite to the flow direction) than to values from the "downwind" direction (in the same direction as the flow) (Adytia & Yuninda, 2020).

Approximation of the value $(uu_x)_j$ using the upwind method is :

$$(uu_x)_j = \begin{cases} u_j^n \left(\dfrac{(u_j^n - u_{j-1}^n)}{\Delta x} \right), & u_j^n \geq 0 \\ u_j^n \left(\dfrac{(u_{j+1}^n - u_j^n)}{\Delta x} \right), & u_j^n < 0 \end{cases} \quad (8)$$

with the water depth $h_{j-1/2} > 0$. This means $u_{j-1/2}$ must be greater than its threshold value. Such a condition is referred to as the Wet-Dry Procedure (Pudjaprasetya, 2018).

Under normal water conditions, it is usually assumed that $\eta(x,0) = 0$ and $u(x,0) = 0$. However, this condition becomes negative in 'dry' areas with $h(x,0) = \eta(x,0) + d(x)$. This can happen because the water depth $d(x)$ in positive in 'wet' regions and $-d(x)$ in 'dry' regions of a domain. Due to the instability of negative h values, the surface deviation height must be modified to $max(0, -d(x))$. Using $max(0, -d(x) + \varepsilon)$ as an infinitely thin layer with thickness ε in 'dry' regions (Pudjaprasetya, 2018).

The following is a scheme with the wet-dry procedure.

$$u_j^{n+1} = \begin{cases} 0, & h_{j-\frac{1}{2}} < \varepsilon \\ u_j^n - \Delta t \left((uu_x)_j + g \dfrac{\eta_{j+\frac{1}{2}}^{n+1} - \eta_{j-\frac{1}{2}}^{n+1}}{\Delta x} \right), & h_{j-\frac{1}{2}} \geq \varepsilon \end{cases} \quad (9)$$

The wet-dry is a method to examine and analyze the effects occurring in a system or process that fluctuates between dry and wet conditions due to changes in water levels.

RESULT AND DISCUSSION

Validation of Wet-Dry Procedure

A. Case for fixed amplitude and varying simulation time

In this section, the simulation aims to validate the numerical method, particularly the wet-dry procedure. This section discusses the wet-dry scheme for wave propagation through dry areas represented by a square bathymetry that emerges above the water surface. The general bathymetric base used is a flat bathymetry with a depth of 2 meters. However, this problem does not have an analytical solution and no experimental data is available. Therefore, validation is ensured by confirming that water can pass through the dry area, waves break on the dry area, and waves are transmitted to the next area, which is a wet area (contains water).

The observation domain spans L = 150m with an initial depth d_0 = -2m. The chosen amplitude is the smallest, A = 0.2m, with a period of T = 5s over varying times of simulation t = 180s, t = 240s, t = 300s, and t = 3s. The period and time were randomly selected.

Table 3. Simulation results of wet-dry with amplitude A = 0.2m over varying times

Amplitude (m)	Period (s)	Time (s)
0.2	5	180
0.2	5	240
0.2	5	300
0.2	5	360

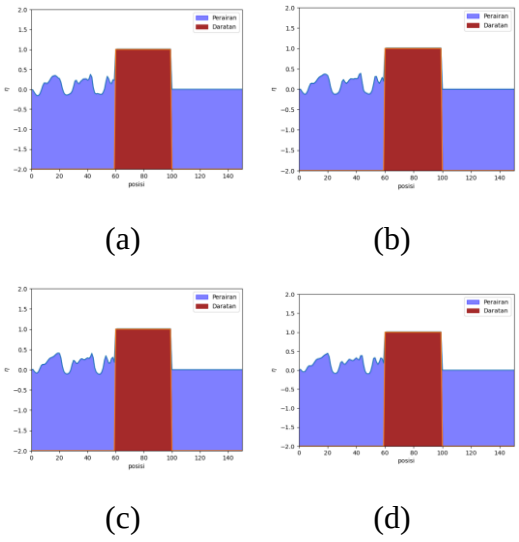

(a) (b)

(c) (d)

Figure 2. Wave propagation with A = 0.2m and T = 5s at (a) 180s, (b) 240s, (c) 300s, (d) 360s long simulation

Based on Figure 2, simulations with amplitude A = 0.2m dan period T = 5s over varying times show that the

waves have not yet reached the land area. Therefore, additional simulations are needed to observe wave conditions that can reach and pass through the land area.

B. Case for fixed simulation time and varying amplitude

Similar to the previous simulation, the observation domain spans L = 150m with an initial depth of d_0 = -2m. The varying amplitudes are A = 0.2m, A = 0.5m, A = 75m, and A = 1m with a period of T = 5s over a time of t = 150s. Amplitude and period data were selected randomly, while the time was chosen because it takes at least 150s to cover the entire observation distance. Below are the simulation results with amplitude variations in Table 4.

Table 4. Simulation results of Wet-Dry with amplitude variations over a time of simulation t = 150s

Amplitude (m)	Period (s)	Time (s)
0.2	5	150
0.5	5	150
0.75	5	150
1	5	150

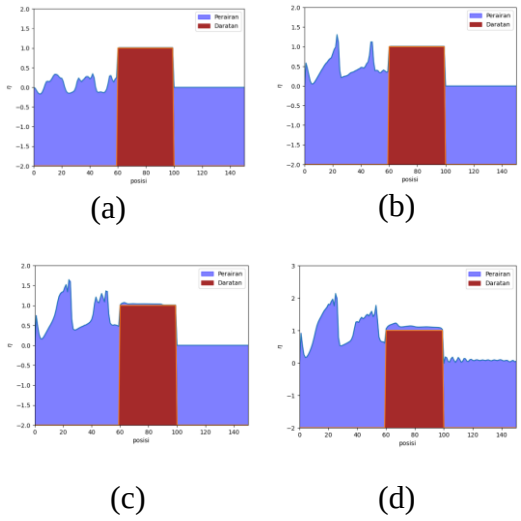

(a) (b)

(c) (d)

Figure 3. Wave propagation with (a) A = 0.2m, (b) A = 0.5m, (c) A = 0.75m, (d) A = 1 m with $\boldsymbol{T}$ = 5s for 150s simulation

Based on Figure 3, in the simulations with an amplitude of A= 0.2m (Figure 3.a) and A = 0.5m (Figure 3.b), the waves could not reach and pass the land area. With an amplitude of A = 0.75m (Figure 3.c), the waves started to reach the land but could not pass through.

However, with an amplitude of A = 1m (Figure 3.d), the waves were able to reach and pass the land area and form incoming waves again up to the observation location. In this wet-dry simulation, with an observation domain of L = 150m a minimum time of t = 150s is required. With the smallest period of T = 5s and different amplitudes, the wave conditions vary in their ability to pass through the land area. In this case, the larger the amplitude, the greater the wave's ability in the water (wet) to reach and pass through the dry or land area.

Simulation of Run Up waves varying amplitudes and fixed period

The observation domain has a length of L= 1144.55 m and a depth of d_0 = -20.8871m (Table 2). In the simulation, a duration of t= 120s is used with varying amplitudes and a fixed period of T = 60s. The amplitudes were randomly selected from the data range that has the closest run-up height (Table 5) to the actual data (Table 1).

Table 5. Simulation results of run-up waves with varying amplitudes and a period of T = 60s

Amplitude (m)	Period (s)	Run up height (m)	Inundation (m)
0.09	60	1.3237	37.0181
0.1	60	1.4224	40.0195
0.11	60	1.5223	43.0210
0.12	60	1.6247	46.0225
0.13	60	1.7288	49.0239
0.14	60	1.8299	52.0254

Based on Table 5, an amplitude of A = 0.09m has an inundation level close to the actual data (Table 1). Conversely, an amplitude of A = 0.14m has run up height close to the actual data (Table 1). The results indicate that with the same period and increasing amplitude, both the run-up height and inundation level increase in the waters around Canti Beach, South Lampung.

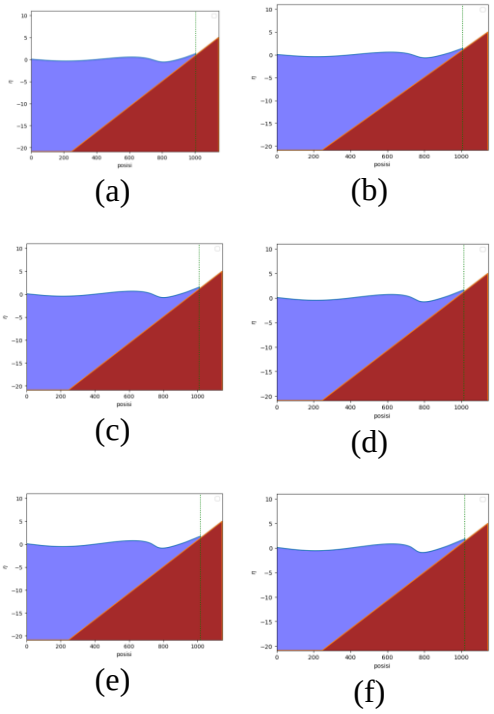

Figure 4. Wave run-up with amplitude variations (a) A= 0.09m, (b) A= 0.1m, (c) A= 0.11m, (d) A= 0.12m, (e) A = 0.13m, and (f) A = 0.14m with $\boldsymbol{T}$ = 5s for 150s simulation

The wave run-up is simulated in Figure 4 with different wave amplitudes, using a staggered grid finite difference method with a wet-dry procedure. As it depicts the flow of water across a slopping bathymetry, this technique performs well at depicting the mechanism of the waves progressing to the beach. These simulations were run using real bathymetry data from Canti Coast, therefore the outcomes are based on the coastal environment. The simulations show how changing wave amplitudes affect the inundation area (distance between the shoreline to the wave run-up) throughout a 150-second simulation period with a wave period of 5 seconds (T = 5 s) by adjusting the amplitude (A) from 0.09 m to 0.14 m. The detailed result can be seen in Table 6.

Table 6. Wavelength with amplitude variations

Amplitude (m)	Wavelength (m)	Maximum surface displacement (m)
0.09	716.3498	0.5367
0.1	716.3498	0.5935
0.11	716.3498	0.6498
0.12	715.3493	0.7050
0.13	715.3493	0.7603
0.14	715.3493	0.8153

Meanwhile, simulations with amplitudes A = 0.12m, A = 0.13m, and A = 0.14m have a wavelength λ = 715.3493m. In this case, the effect of amplitude variations on the wavelength is not significant. The wavelength tends to have small differences or even be the same at some successive amplitudes.

Simulation of Run Up waves with constant amplitude and varying period

The observation domain remains at a distance of L = 1144.5590m and a depth of d_0 = -20.8871m (Table 2). In the simulation, a time of simulation of t = 120s is used with the maximum amplitude of A = 0.14m and varying periods. This amplitude was chosen because it provides a run-up height (Table 5) that most closely matches the actual data (Table 1).

p-ISSN 1829 586X
e-ISSN 2581-0170

Table 7. Results of the run-up waves simulation with varying amplitude and a period of T = 60s

Amplitude (m)	Period (s)	Run up height (m)	Inundation (m)
0.14	30	1.3206	43.0210
0.14	40	1.4950	45.0220
0.14	50	1.6427	47.0230
0.14	70	1.8169	49.0239
0.14	80	1.8976	50.0244
0.14	90	1.8739	48.0235

Based on Table 7, the amplitude of A = 0.14m with period T = 70s and T = 90s has a run-up height that closely matches the actual data (Table 1). Conversely, the amplitude of A = 0.14m with a period of T = 30s has an inundation that closely matches the actual data (Table 1). Based on the results obtained, with the same amplitude and increasing period, there is still a decrease in the values of run-up height and inundation, particularly at a period of T = 90s. The run-up simulation can be seen in Figure 5.

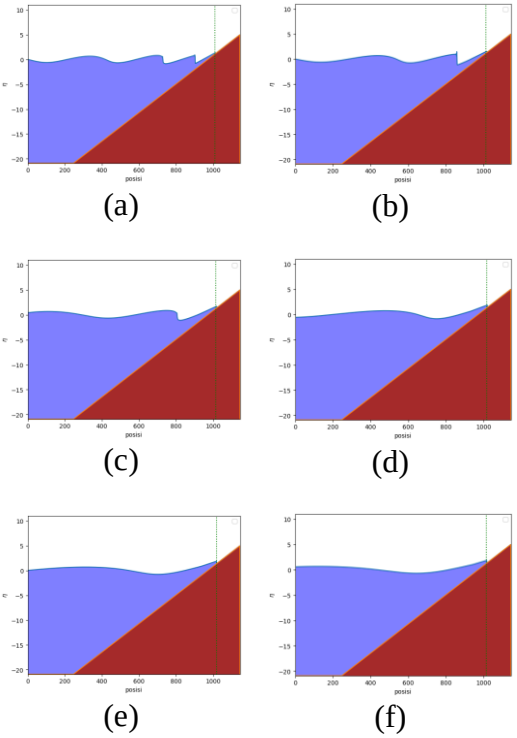

Figure 5. Run up waves with varying period (a) T = 30s, (b) T = 40s, (c) T = 50s, (d) T = 70s, (e) T = 80s, and (f) T = 90s

Table 8. Wavelength with varying period

Period (s)	Wavelenghth (m)	Maximum displacement (m)
30	174.0850	1.0244
40	320.1563	0.8984
50	513.2506	0.8591
70	873.4149	0.9414
80	849.4149	0.9245
90	819.4003	0.9025

The following is the graph of wavelength with period variations.

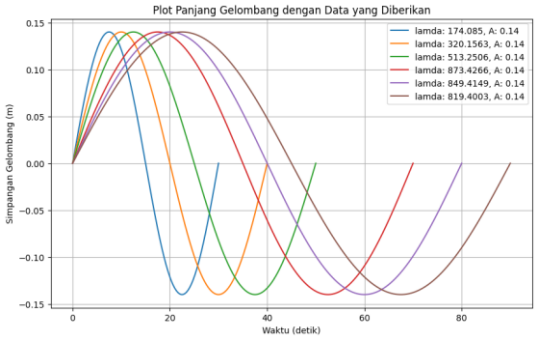

Figure 6. Wavelength with varying period

Based on the graph in Figure 6, it is known that the simulation with a period of T = 30s has the shortest wavelength λ = 174.0850m. The details are in Table 8. The period of T = 70s has the longest wavelength λ = 873.4266m. Subsequently, there is a decrease in the wavelength values from the period of T = 80s to T = 90s, measuring 849.4149m and 819.4003m, respectively. In this case, with a constant amplitude and increasing period over t = 120s, the wavelength within 1 period may not be fully observed due to the excessively large period given.

CONCLUSION

The simulation of the run-up wave phenomenon at Canti Beach, South Lampung, has been conducted by using real bathymetric data and a Nonlinear Shallow Water Equation (SWE) model.

p-ISSN 1829 586X
e-ISSN 2581-0170

The simulation aimed to validate the numerical method, particularly the wet-dry procedure, to ensure accurate wave propagation through dry and wet areas. The simulation shows that the wet-dry procedure was successfully applied so that waves with certain amplitudes (A = 0.2m and A = 0.5m) could reach and pass the dry land area, then the transmitted wave became incoming waves again in the wet area. This confirms the wet-dry scheme's ability to model wave behavior in simple bathymetric conditions.

Additionally, the results indicated that both run-up height and inundation levels increased with increasing wave amplitude. Specifically, an amplitude of A = 0.09m produced an inundation level close to the actual observed data obtained from post tsunami event, while an amplitude of A = 0.14m yielded a run-up height close to the observed data. This suggests that higher amplitudes result in more significant wave impacts on the shore.

Simulations with an amplitude A = 0.14m and varying periods showed that periods of T = 70s and T = 90s closely matched the observed run-up height, while a period of T = 30s matched the observed inundation level. This highlights the period's influence on wave behavior, with longer periods resulting in decreased run-up height and inundation values.

Overall, this study demonstrates the implementation of a numerical model of shallow water model with a wet-dry scheme to simulate and predict run-up wave behavior and inundation areas. Thus, we can reconstruct the physical characteristics of the tsunami. Specifically, we are concentrating on estimating the wave amplitude and frequency at the time of the occurrence. As there are no direct observations of the approaching tsunami waves, our method makes use of the run-up and flooding field data that the Indonesian Meteorology, Climatology, and Geophysical Agency (BMKG) quickly collected following the disaster. This result can be used to identify the potential wave scenarios that could have resulted in the observed effects by doing back calculations using the observed run-up heights and inundation extents. By improving early warning systems and coastal defences and understanding the dynamics of the tsunami, this information will help reduce the impact of future tsunamis in the area.

REFERENCES

Adytia, D., & Yuninda, A. P. (2020). Pendekatan numerik disipasi gelombang reguler oleh hutan mangrove menggunakan model dispersif boussinesq. *Jurnal Ilmu Dan Teknologi Kelautan Tropis*, *12*(1), 53–67. https://doi.org/10.29244/jitkt.v12i1.26328

Arifin, A. Z. (2021). Simulasi Dampak Penghalang pada Gelombang Tsunami Menggunakan Persamaan Air Dangkal dengan Metode Beda Hingga. *Jambura Journal of Mathematics*, *3*(2), 93–102. https://doi.org/10.34312/jjom.v3i2.10068

Azdy, R. A., & Darnis, F. (2020). Use of haversine formula in finding distance between temporary shelter and waste end processing sites. *Journal of Physics: Conference Series*, *1500*(1), 012104. https://doi.org/10.1088/1742-6596/1500/1/012104

Busayo, E. T., & Kalumba, A. M. (2020). Coastal Climate Change Adaptation and Disaster Risk Reduction: A Review of Policy, Programme and Practice for Sustainable Planning Outcomes. *Sustainability*, *12*(16), 6450. https://doi.org/10.3390/su12166450

Campbell, J. R. (2022). From the Frying Pan into the Fire? Climate Change,

Urbanization and (In)Security in Pacific Island Countries and Territories. *Peace Review*, 1–11. https://doi.org/10.1080/10402659.2022.2023425

Cummins, P. R., Pranantyo, I. R., Pownall, J. M., Griffin, J. D., Meilano, I., & Zhao, S. (2020). Earthquakes and tsunamis caused by low-angle normal faulting in the Banda Sea, Indonesia. *Nature Geoscience*, *13*(4), 312–318. https://doi.org/10.1038/s41561-020-0545-x

Fauzi, R., & Wiryanto, L. H. (2017). On the staggered scheme for shallow water model down an inclined channel. *AIP Conference Proceedings*. https://doi.org/10.1063/1.4994405

Fauzi, R., & Wiryanto, L. H. (2021). Momentum conservative scheme for simulating granular landslide over an inclined rigid bed. *Advances and Applications in Fluid Mechanics*, *27*(1), 37–45. https://doi.org/10.17654/fm027010037

Fauzi, R., & Wiryanto, L. H. (2023). Numerical simulation of granular landslide using predictor-corrector method. *AIP Conference Proceedings*. https://doi.org/10.1063/5.0166775

Goyman, G. S., & Shashkin, V. V. (2021). Horizontal approximation schemes for the staggered reduced latitude-longitude grid. *Journal of Computational Physics*, *434*, 110234–110234. https://doi.org/10.1016/j.jcp.2021.110234

Sabara, Z., Umam, R., Prianto, K., Junaidi, R., & Rahmat, A. (2021). Anak Krakatau mountain (AKM) causes a rare tsunami phenomenon: Impact around the Sunda Strait, Indonesia. *IOP Conference Series: Earth and Environmental Science*, *739*(1), 012036. https://doi.org/10.1088/1755-1315/739/1/012036

Sianturi, G. S., & Fauzi, R. (2023). Pemodelan kedalaman laut pada perairan selat sunda dan sekitarnya menggunakan neural network. *Prosiding Seminar Nasional Sains Dan Teknologi "SainTek," 1*(1), 1–11. https://conference.ut.ac.id/index.php/saintek/article/view/2285

Sri Redjeki Pudjaprasetya. (2018). Transport Phenomena, equations, and numerical methods. *INA-Rxiv (OSF Preprints)*. https://doi.org/10.31227/osf.io/5vw73

Sugiarto, A., Rudianto, & Somali, L. (2018). *Laporan survey tsunami selat sunda wilayah Lampung*.

Tiwi, D. A., N Sudiana, None Prihartanto, I Turyana, F Prawiradisastra, Q Zahro, & None Astisiasari. (2023). Post-disaster rapid assessment of Sunda Strait tsunami on 24–25 December 2018 in the regencies of serang and Pandeglang, province of Banten, Indonesia. *IOP Conference Series. Earth and Environmental Science*, *1173*(1), 012015–012015. https://doi.org/10.1088/1755-1315/1173/1/012015

Tursina, Syamsidik, Kato, S., & Afifuddin, M. (2021). Coupling sea-level rise with tsunamis: Projected adverse impact of future tsunamis on Banda Aceh city, Indonesia. *International Journal of Disaster Risk Reduction*, *55*, 102084. https://doi.org/10.1016/j.ijdrr.2021.102084

Wang, X., Qiao, D., Jin, L., Yan, J., Wang, B., Li, B., & Ou, J. (2023). Numerical investigation of wave run-up and load on heaving cylinder subjected to regular waves. *Ocean Engineering*, *268*, 113415. https://doi.org/10.1016/j.oceaneng.2022.113415